Carbon Vol. 22, No. 3, pp. 253-263, 1984
Printed in Great Britain

0008-6223/84 $3.00 + .00

EXFOLIATION OF INTERCALATED GRAPHITE†

S. H. ANDERSON and D. D. L. CHUNG
Department of Metallurgical Engineering and Materials Science, Carnegie-Mellon University, Pittsburgh, PA 15213, U.S.A.

(*Received* 1 *February* 1983)

Abstract—By X-ray diffraction, exfoliated graphite–Br_2 was found to exhibit the same in-plane superlattice ordering as intercalated graphite prior to exfoliation. This ordering persisted even after heating for 1 hr at 1700°C. By dilatometry, a single exfoliation event was found to consist of multiple expansion spurts, which occurred at ~150 and ~240°C for the first exfoliation, and ~100 and ~240°C for subsequent cycles. The amount of expansion was found to increase with decreasing intercalate activity during intercalation. With exfoliation cycles to higher temperatures or longer times, the amount of residual expansion after the collapse on cooling increased until no second exfoliation was observed or reheating. Due to intercalate desorption, the amount of expansion for concentrated samples increased with increasing sample width; desorbed samples showed little width dependence. Acoustic emission was observed before appreciable expansion during the first exfoliation cycle; it was not observed during the collapse or subsequent exfoliation cycles. A model of exfoliation involving intercalate islands is proposed.

1. INTRODUCTION

When intercalated graphite is heated past a critical temperature, a large expansion along the *c*-direction occurs, giving the compound a puffed-up appearance. This phenomenon is known as exfoliation.

Brocklehurst[1] observed by dilatometry that desorbed graphite–Br_2 based on polycrystalline artificial extruded graphite began exfoliation at ~300°C upon heating, resulting in an expansion of up to ~2.1% at 500°C. By similar dilatometric measurement on desorbed graphite–Br_2 based on pyrolytic graphite, Martin and Brocklehurst[2] found that

1. first exfoliation occurred at ~170°C upon first heating,
2. subsequent exfoliation occurred at ~120°C in subsequent heating cycles,
3. collapse occurred at ~110°C upon cooling,
4. second and subsequent exfoliation cycles were reversible,
5. the expansion was up to 380% at 500°C,
6. the exfoliation temperature increased linearly with increasing load.

In contrast to the relatively small amount of expansion observed by Martin and Brocklehurst[2], and Ubbelohde[3] observed an expansion of ~1000% at 350°C for graphite–Br_2 based on well-oriented graphite. By using differential thermal analysis, optical microscopy and gaseous pycnometry, Mazieres *et al.*[4] found that desorbed graphite–Br_2 based on pyrocarbons underwent first exfoliation at 160–200°C on heating, second exfoliation at 100–120°C on heating, and collapse at 70–100°C on cooling. Furthermore, they found that thermal cycling decreased the exfoliation tendency progressively and that this effect was more pronounced when the heating was carried out in air. Mazieres *et al.*[5] observed irreversible exfoliation after heating desorbed graphite–Br_2 based on pyrocarbons to 1000°C and cooling in an argon atmosphere. In addition, they demonstrated that it was possible to intercalate the irreversibly exfoliated material.

Other than graphite–Br_2, exfoliation had also been observed in graphite-ferric chloride[6], graphite-aluminum chloride[7], and graphite intercalated with a mixture of nitric and sulfuric acids[7].

The tendency for exfoliation depends on the extent of stacking order of the graphite basal planes[8]. Dowell[9] showed that possession of a basal plane stack height, L_c, greater than ~450 Å was necessary for exfoliation.

The exfoliation phenomenon is of technological importance as well as scientific interest. The exfoliation of graphite–HNO_3–H_2SO_4 has been used to manufacture Grafoil[10], a high temperature gasket and packing material. The exfoliation of graphite–HNO_3–H_2SO_4 has been used for making a thermal insulator for molten metals[11]. The exfoliation of graphite–$FeCl_3$–NH_3 has been used for making blankets for the extinction of metal fires[12]. In addition, exfoliated graphite is being investigated by the U.S. Army for use as a battlefield obscurant[13]. The surface area increase resulting from irreversible exfoliation is attractive for catalytic applications of graphite intercalation compounds[14]. In addition, exfoliation is a phenomenon that affects the thermal stability of graphite intercalation compounds, so understanding of this phenomenon is necessary for the use of graphite intercalation compounds at elevated temperatures.

---

†Research sponsored by the Air Force Office of Scientific Research, Air Force Systems Command, USAF, under Grant No. AFOSR-78-3536. The United States Government is authorized to reproduce and distribute reprints for governmental purposes notwithstanding any copyright notation hereon.

Martin and Brocklehurst[2], and Aoki *et al.*[15] both modeled the exfoliation of graphite–bromine by considering the expansion of gaseous bubbles as Griffiths cracks, though Aoki *et al.*[15] treated intercalated bromine at room temperature as a solid which vaporized at the breakaway temperature. Both assumed the bubbles to be trapped at defects within the crystal. Setton[4] also modeled the exfoliation of graphite–bromine as the vaporization of condensed phase, after the migration of bromine to defects. Olsen *et al.*[16], in a study of the exfoliation of graphite–bisulfate compounds, proposed that a bisulfate compound existed as pockets at grain boundaries, with much of the graphite remaining unaffected. They proposed that the intercalate vaporized on heating, in effect causing the pockets to explode, leaving a low density, "isotropic" material between planar arrays of pyrolytic graphite and voids. Similarly, Stevens *et al.*[6] viewed exfoliation of graphite–ferric chloride as the forcible rupture of sealed or partially sealed spaces within graphite due to the fact that ferric chloride decomposed to iron and chlorine gas. Dowell[7], in discussing the structures of exfoliated graphite–bisulfate and graphite–aluminum chloride compounds, agreed that the intercalate should diffuse to defects to form three-dimensional aggregates which could vaporize, expanding the structure. He also suggested channels through which the vapor escaped from the sample.

While it is clear that exfoliation is due to the expansion of the intercalate in gas-filled cells, the origin of such gas-filled cells remains unclear. The suggestion of segregation to defects begs the question of the nature of the defects. Grain boundaries[16] may serve as segregation sites, but our finding[17] that single crystal graphite–bromine exfoliates more easily than the HOPG counterpart does not support the suggestion that these are the origins of the gas cells. We have reported that the exfoliation behavior depends more strongly on the parent initial stage than on the intercalate concentration in graphite–Br_2[18]. This paper supports this contention and offers further insight into the exfoliation process. The key issues which are addressed include the following. Is exfoliated graphite still intercalated? How does exfoliation affect the structure of the parent graphite or the intercalation compound? How reversible is exfoliation? How can the reversibility or irreversibility of exfoliation be controlled? What is the mechanism of exfoliation?

In this work, we have used dilatometry to investigate the dependence of multiple exfoliation and collapse on the stage, the intercalate concentration, the intercalation temperature, the annealing time and temperature after the first exfoliation, the sample size, and the intercalate species. Particular attention was given to the reversibility of exfoliation. In addition, acoustic emission was used to investigate the nature of the exfoliation process and X-ray diffraction was used to study the crystal structure of the exfoliated material.

The main findings of this work are the following.

(1) Exfoliated graphite exhibits the same in-plane superlattice ordering as intercalated graphite prior to exfoliation. This ordering persists even after heating for an hour at 1700°C.

(2) Acoustic emission was observed before appreciable expansion during the first exfoliation cycle. It was not observed during the collapse or subsequent exfoliation cycles.

(3) A single exfoliation event consists of multiple expansion spurts, which occur at ~150° and ~240°C for first exfoliation, and at ~100° and ~240°C for subsequent cycles.

(4) The expansion was found to increase with decreasing intercalate chemical activity during intercalation such that it increased with decreasing Br_2 concentration in the Br_2–CCl_4 solution and with increasing intercalation temperature.

(5) In samples heated to high temperatures and/or held for extended times at high temperatures, the amount of residual expansion after the collapse on cooling increased until no second exfoliation was observed on reheating, i.e. exfoliation became irreversible.

(6) Due to intercalate desorption, concentrated intercalated graphite shows more expansion after first exfoliation than after second exfoliation. However, desorbed intercalated graphite shows less expansion after first exfoliation than after second exfoliation.

(7) On repeated exfoliation-collapse cycles (also called exfoliation cycles), concentrated samples show a decrease in the amount of expansion due to desorption during exfoliation, while desorbed samples show little decrease in the amount of exfoliation.

(8) Due to intercalate desorption, the amount of expansion for concentrated samples increases with increasing sample width. However, desorbed samples show little width dependence.

2. EXPERIMENTAL TECHNIQUES

Samples were prepared from highly oriented pyrolytic graphite (HOPG) kindly provided by Union Carbide Corporation. Most samples were cut to a size of 4 mm × 4 mm × 0.5 mm and then placed in liquid bromine for intercalation. Samples which were intercalated above room temperature were placed in a constant temperature bath. Times of the order of a minute were required to place a sample in a sample holder, add bromine, seal the sample holder and place it in the water bath. A similar amount of time was necessary to remove the sample from the bath, quench it to room temperature, and remove the sample from the bromine. Fourth stage samples were prepared by placing the samples in a 15 mol% Br_2 bromine–carbon tetrachloride solution. A 12 mm × 12 mm × 1 mm sample of graphite was intercalated in pure bromine for intercalation to second stage and was then cleaved and cut to produce pairs of 7 mm × 7 mm, 5 mm × 5 mm and 2 mm × 2 mm samples. Half the samples was reimmersed in bromine until exfoliation; the other half was allowed to desorb. Desorption of the lamellar compounds was allowed to occur in air or nitrogen. Stage 1 graphite–ICl was prepared by immersion of HOPG in ICl liquid at room temperature. The stage of all samples was characterized by X-ray diffractometry using Cu $K\alpha$ radiation.

The effect of exfoliation on the intercalate in-plane superlattic was investigated by X-ray diffraction. The Transmission Laue Method was used, with Mo K_α radiation and a specimen-to-film distance of 6 cm. The samples were oriented to yield mainly the (hkO) in-plane diffraction lines. The set-up allowed d-values ranging from 0.8 to ~6 Å to be measured. The exposure time was ~12 hr for every sample.

Exfoliation expansion was followed with a probe connected to a linear variable differential transducer (LVDT). The sample was heated by a furnace around the support extending an inch above the sample. As a consequence of active cooling of the support, the air surrounding the sample was hotter than the support surface. This had the result that when exfoliation started, the sample temperature increased toward the ambient air temperature due to enhanced insulation from the cooler support. The sample temperature was measured by a Pt–Pt 10% Rh thermocouple bead in contact with the sample. A heating and cooling rate of 20°C/min was used in the exfoliation cycles. The weight of the probe on the sample was 28 g. The samples were purged with nitrogen gas in the presence of air during the measurements.

Acoustic emission during exfoliation was detected by using an ultrasonic transducer (Aerotech Gamma, 1.6 MHz narrow band or 0.5 MHz wideband) equipped with a high temperature delay line. The transducer signal was amplified and the acoustic emission pulses were counted by using a frequency counter.

3. EXPERIMENTAL RESULTS

Figure 1 shows X-ray diffraction patterns obtained on graphite–Br_2 (a) after desorption from saturation and before exfoliation, and (b) after exfoliation carried out at ~300°C. The indexing of the diffraction lines are shown in Table 1 for these samples as well as pristine graphite and graphite–Br_2 exfoliated at 1700°C. The in-plane superlattice was the same as that of stage 2 graphite–Br_2 based on single crystal graphite, as determined by Ghosh and Chung[19]. The unit cell is monoclinic and commensurate with the graphite lattice, with in-plane lattice constants $a = 4.26$ Å, $b = 8.87$ Å, and the angles $\alpha = \beta = 90°$ and $\gamma = 103.9°$. Due to the mechanical deformation resulting from exfoliation, the diffraction pattern was closer to a powder pattern after exfoliation, as indicated by the complete diffraction rings obtained after exfoliation (Fig. 1). For the same reason, certain (hkl) lines not observed before exfoliation were observed afterward.

Figure 2 illustrates the general features of exfoliation which we observed in graphite–Br_2 by dilatometry. The sample (5 × 5 mm) was initially intercalated to 3.2 mol% Br_2 (stage 4), desorbed to 1.3 mol% Br_2, reintercalated to 6.3 mol% Br_2 (stage 2), and desorbed to 1.6 mol% Br_2. During the initial part of the first heating cycle, expansion occurred very slightly though with a thermal expansion coefficient several times that of graphite. Eventually the sample exfoliated within a relatively narrow temperature range. We have determined a first onset temperature (T_1 for the first exfoliation cycle, T_2 for the second cycle) by extrapolating the line of exfoliation expansion and taking its intersection with the horizontal base line. The expansion rate diminished to form a shoulder (first shoulder) in the curve, and then increased again to form a second shoulder, as shown in Fig. 2, where the second shoulder of the first exfoliation cycle is labeled. No shoulders were observed at higher temperatures up to 600°C in graphite–Br_2. We designate the fractional expansion at the first shoulder as E_1 for the first cycle and E_2 for the second cycle, as determined by the intersection of the line of exfoliation expansion and the expansion line at the shoulder. The second onset temperature and the fractional expansion at the second shoulder

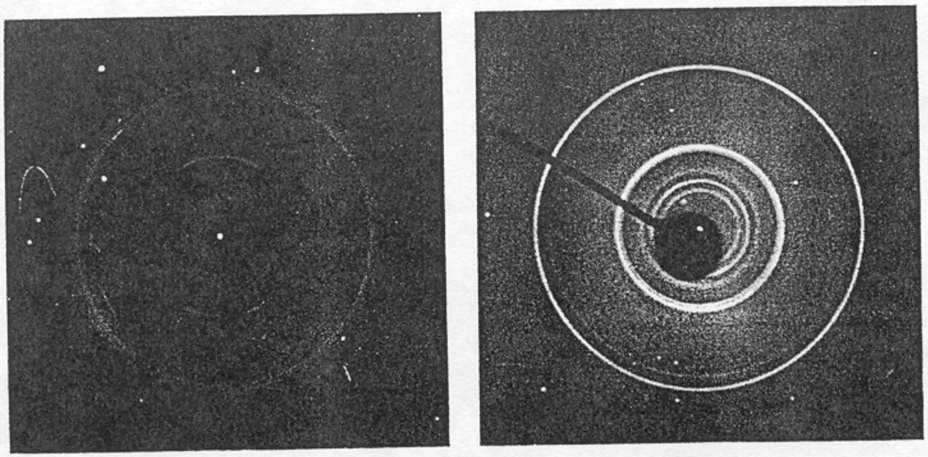
(a) (b)

Fig. 1. Transmission Laue X-ray diffraction patterns of graphite–Br_2 (HOPG) (a) after desorption from saturation and before exfoliation, and (b) after exfoliation carried out at ~300°C.

Table 1. X-Ray diffraction lines of pristine graphite, desorbed graphite–bromine and exfoliated graphite–bromine

hkl	Pristine graphite			Graphite-Br_2, desorbed			Graphite-Br_2, exfoliated at 300°C			Graphite-Br_2, exfoliated at 1700°C		
	d_{obs} (Å)	d_{cal} (Å)	Strength	d_{obs} (Å)	d_{cal} (Å)	Strength	d_{obs} (Å)	d_{cal} (Å)	Strength	d_{obs} (Å)	d_{cal} (Å)	Strength
023_G							0.96	0.96	VW			
016_G							0.99	0.99	VW	0.99	0.99	VW
$200_G(260)_S$	1.09	1.07	W	1.09	1.07	W						
112_G							1.15	1.13	S	1.15	1.13	M
$110_G(700)_S$	1.25	1.23	M	1.26	1.23	M	1.23	1.23	W	1.23	1.23	M
011_G							2.03	2.03	VS	2.02	2.03	S
$100_G(130)_S$	2.14	2.13	M	2.14	2.13	M	2.14	2.13	M	2.14	2.13	M
120_S							2.66	2.68	W	2.73	2.68	VW
300_S				2.85	2.87	W	2.88	2.87	W	2.86	2.87	VW
002_G							3.36	3.35	S	3.39	3.35	S
200_S				4.16	4.14	W	4.17	4.14	W			

G = graphite
S = in-plane superlattice

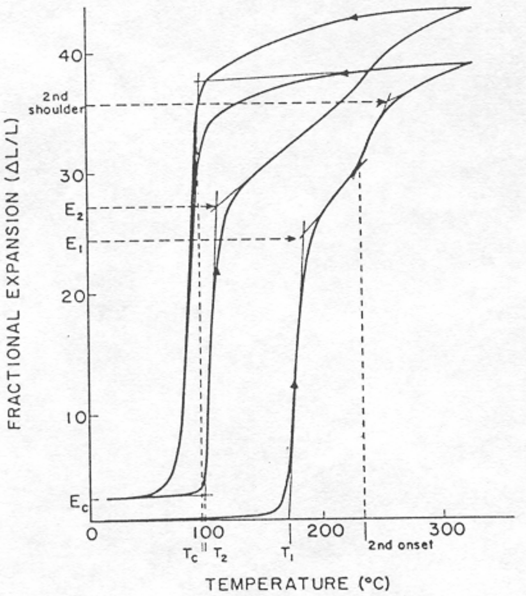

Fig. 2. Fractional expansion vs temperature during the first two exfoliation-collapse cycles for graphite–Br_2 (HOPG) which had been desorbed form 3.2 mol% Br_2 to 1.3 mol% Br_2, then reintercalated to 6.3 mol% Br_2 and desorbed to 1.6 mol% Br_2 prior to heating.

are illustrated in Fig. 2 for the first exfoliation cycle. On cooling, a large degree of hysteresis was evident, with contraction of the exfoliated structure occurring predominantly within a narrow temperature range, resulting in a small residual fractional expansion, E_c. We designate the collapse temperature T_c as the temperature determined by the intersection of lines extrapolated from the contraction region and the linear region of the curve on cooling prior to collapse. On reheating, second exfoliation occurred at about the same temperature at which collapse occurred during cooling, i.e. $T_2 = T_c$. It is interesting to note that while T_1 and T_2 were quite separate, the second shoulder was observed at about the same temperature in any exfoliation cycle. The collapse behavior was largely the same for any exfoliation cycle.

The exfoliation behavior of a first stage graphite–ICl (HOPG, 4 × 4 mm) is shown in Fig. 3. In general the exfoliation curve is much like that observed for graphite–Br_2. The main difference is that the exfoliation onset temperature T_1 of graphite–ICl is approximately the same as the collapse temperature T_c and the second exfoliation temperatures T_2, whereas in graphite–Br_2. T_1 is generally higher than T_2. It may also be pointed out that T_2 in graphite–ICl is about 100°C higher than that of graphite–Br_2.

In comparing Figs. 2 and 3, it can be seen that the amount of expansion which occurred during second exfoliation of graphite–ICl was considerably less than that which occurred in graphite–Br_2. This is probably not an attribute of the intercalate species, but rather a consequence of the amount of desorption which had occurred during first exfoliation. While the graphite–ICl sample was a saturated (first stage) compound just before exfoliation was begun, the graphite–Br_2 sample was a desorbed sample prior to exfoliation. Therefore, desorption was much more significant during first exfoliation of the graphite–ICl

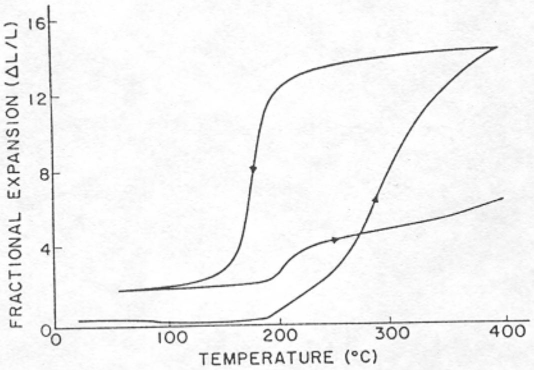

Fig. 3. Fractional expansion vs temperature during the first one and a half exfoliation-collapse cycles for graphite–ICl (HOPG) which was saturated (stage 1) prior to heating.

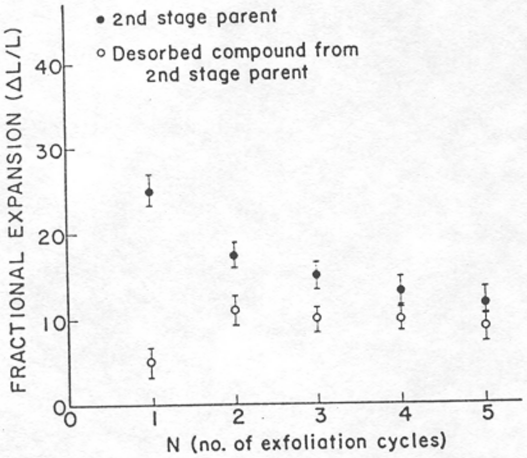

Fig. 4. Fractional expansion at the first shoulder (E_N) vs the number of exfoliation cycles (N) for graphite–Br_2 (HOPG) which (i) were not desorbed prior to heating and (ii) were desorbed prior to heating.

sample than the graphite–Br_2 sample. The dependence of exfoliation on desorption is given later in this paper.

Figure 4 illustrates the dependence of expansion on the number, N, of exfoliation cycles for 5 mm × 5 mm graphite–Br_2 samples which were, in one case (open circles), allowed to desorb from a second stage parent compound to 1.5 mol% Br_2 before exfoliation and, in the other case (closed circles), not allowed to desorb before exfoliation (i.e. the second stage parent compound). The fractional expansion at the first shoulder (i.e. E_N, where N is the number of exfoliation cycles) was plotted vs N. At the end of five exfoliation cycles, each carried out to 290°C, the partially desorbed sample had further desorbed to 0.7 mol% Br_2. For the desorbed sample, E_2 was greater than E_1, and there was only a slight decrease from E_2 to E_5. For the second stage parent compound, the bromine concentration varied from 6.3 mol% Br_2 before the first exfoliation run to 0.6 mol% Br_2 after the fifth exfoliation cycle, each carried out to 340°C. In this case, the expansion behaved as might be expected, i.e., $E_1 > E_2 > E_3 > E_4 > E_5$. In general, we observed $E_1 > E_2$ when samples were exfoliated without prior desorption, and $E_1 < E_2$ when samples were allowed to desorb to an approximately constant weight before exfoliation.

The extent of desorption during each exfoliation cycle was measured by gravimetry. The results are shown in Fig. 5, where the intercalate concentration (in mol% Br_2) was plotted against the square root of the number, N, of exfoliation cycles. The sample (2 × 2 mm) had been desorbed from second stage to 1.4 mol% Br_2 prior to exfoliation. The greatest weight loss occurred during the first and second exfoliation cycles, with the concentration decreased from 1.4 to 1.2 mol% Br_2 after the first exfoliation and from1.2 to 0.9 mol% Br_2 after the second exfoliation. A similar loss, from 0.9 to 0.7 mol% Br_2 required seventeen additional exfoliation cycles. It is this region from $N = 2$ to $N = 19$ which is shown in Fig. 5. The concentrations after cycles 0 and 1 are not shown because they are too far from the subsequent concentrations. The line drawn is a least square fit of the data with a correlation coefficient of -0.96. The dependence on $\sqrt{N}$ suggests that the weight loss may be treated as a diffusion process with an exfoliation cycle being analogous to a unit of desorption time. The effective overall diffusion coefficient during an exfoliation cycle is probably an average of the diffusion coefficients within the temperature range covered by the exfoliation cycle.

Figure 6 shows the dependence of E_1 on the sample width (the dimension perpendicular to the c-axis) for samples which were initially second stage. The filled circles correspond to samples which were not desorbed prior to exfoliation, and the open circles correspond to samples which were allowed to desorb to ~1.5 mol% Br_2 before the exfoliation cycles. The samples were all square and of approximately the same thickness. For samples which were not allowed to desorb, E_1 increased as the width of the sample

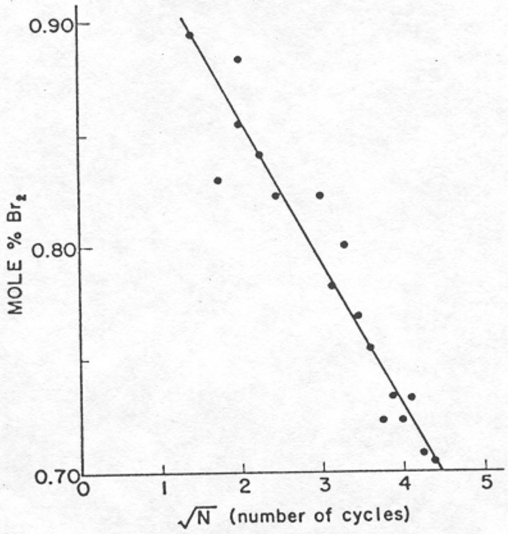

Fig. 5. Gravimetric determination of the intercalate (Br_2) concentration in HOPG as a function of $\sqrt{N}$, where N is the number of exfoliation cycles.

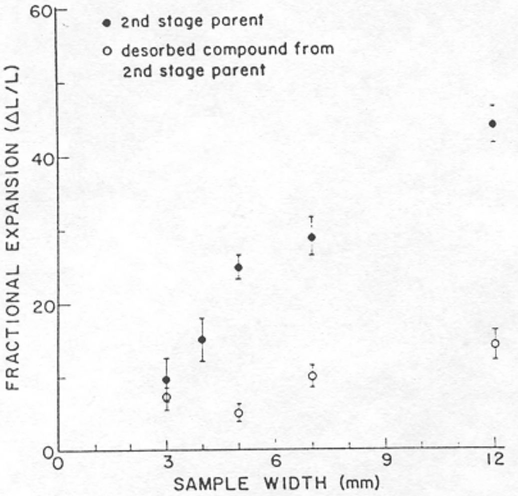

Fig. 6. Fractional expansion at the first shoulder during first exfoliation (E_1) vs the sample width perpendicular to the c-axis for graphite–Br_2 (HOPG).

increased. The samples which were allowed to desorb did not show this size dependence. Consequently we attribute the apparent width dependence to actually a concentration dependence, which is appearing as a consequence of desorption during the previous exfoliation cycles. This point is discussed in the next section.

Figure 7 illustrates the effect of the maximum temperature on the exfoliation behavior. The samples (4 × 4 mm) were intercalated to 6.3 mol% Br_2 (stage 2), but not allowed to desorb before heating. Plot *A* in Fig. 7 shows dilatometric results obtained during two exfoliation cycles carried out to ~200°C; Plot *B* was obtained during two cycles carried out to ~400°C; Plot *C* was obtained during two cycles carried out to ~600°C. The main trend indicated in Fig. 7 is that E_c (the residual fractional expansion) increased as the maximum temperature increased. Figure 8 shows similar effects due to isothermal annealing at the maximum temperature during the first heating. Contraction was observed during annealing. After annealing for 0.5 hr at ~600°C, the fractional expansion was only 90% of the initial 600°C expansion; after a 1 hr anneal, the fractional expansion was 80% of the initial 600°C expansion; after a 3-hr anneal, the fractional expansion was 70% of the initial 600°C expansion. However, no contraction was observed in samples annealed at 200 or 400°C. It should be noted that a second exfoliation was not observed in the samples annealed at 600°C. The results of annealing at different temperatures for various lengths of time are summarized in Table 2, where E_c and E_2 are listed relative to E_1 to lower the effect of the error in measuring the initial sample thickness. Whereas E_c/E_1 is affected by annealing, E_2/E_1 appears independent of annealing. While most of the data were obtained at heating rates of 20°C/min, several runs were made at 10 and 40°C/min. Within this range of heating rates, little or

Table 2. Effect of annealing on exfoliation behavior

Annealing Temperature (°C)	Annealing Time (hr.)	E_c/E_1	E_2/E_1	Contraction at T_{max}
200	0	0.09	0.60	0
	0.5	0.14	0.42	0
	1	0.20	0.54	0
400	0	0.16	0.51	0
	0.5	0.20	0.61	0
	1	0.31	0.49	0
600	0	0.44	0.58	0
	0.5	0.59	0.59	10%
	1	0.67	0.67	20%
	3	0.74	0.74	30%

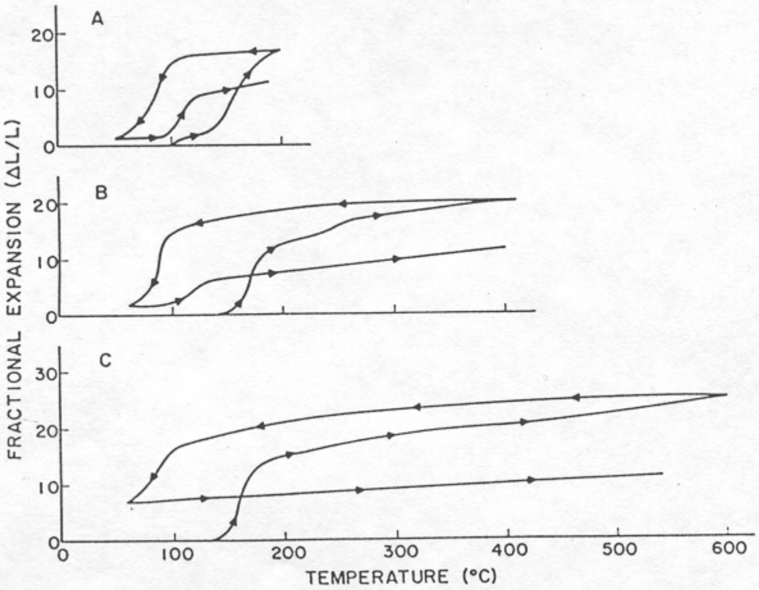

Fig. 7. Fractional expansion vs temperature during the first one and a half exfoliation-collapse cycles carried out to three different maximum temperatures for graphite–Br_2 (HOPG).

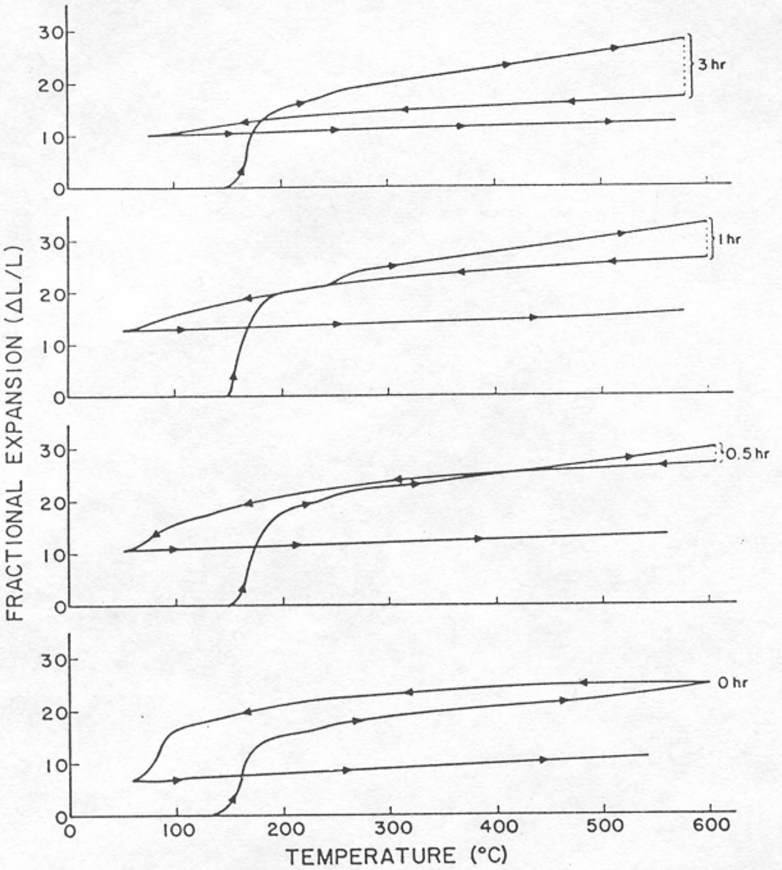

Fig. 8. Fractional expansion of graphite–Br_2 (HOPG) vs temperature during the first one and a half exfoliation-collapse cycles in which isothermal annealing at the maximum temperature (~600°C) during the first heating cycle was carried out for various lengths of time.

no effects were observed which could be attributed to the change in heating rate. This is most likely due to the fact that even at 40°C/min, the time spent in heating to the exfoliation temperature is long compared to the time needed for desorption.

We have previously reported that the initial stage determines the exfoliation behavior[18]. We have further evidence that the initial intercalating conditions determine the exfoliation behavior. Table 3 illustrates the effect of the initial stage on the subsequent exfoliation behavior. Some samples were allowed to be intercalated, desorbed and reintercalated. Irrespective of the stage after the second intercalation, the samples which were first inter-

Table 3. Effect of staging on exfoliation behavior

Stage after 1st intercalation	4	4	2	2
Stage after 2nd intercalation	2	*	4	*
Mole % Br_2	1.60	1.39	1.55	1.53
First exfoliation				
Temperature T_1 (°C)				
1st onset	161	145	185	185
2nd onset	239	230	230	223
Fractional expansion (ΔL/L)				
1st shoulder (E_1)	28	18	8	5
2nd shoulder	39	23	20	14
First collapse				
Temperature T_c (°C)	101	89	104	105
Residual fractional expansion (E_c)	2.3	1.1	2.1	1.0
Second exfoliation				
Temperature T_2 (°C)	100	99	99	108
Fractional expansion (E_2)	30	16	15	11

* Not applicable because 2nd intercalation was not performed.

calated to fourth stage in a Br_2–CCl_4 solution of 15 mol% Br_2 had a lower T_1, larger E_1 and larger E_2 than those which were first intercalated to second stage. Within a group of the same initial stage, the sample intercalated twice had a greater E_1 and E_2 than the sample intercalated once, though neither T_1, T_c nor T_2 were affected by reintercalation.

Table 4 is a list of E_1 for samples intercalated in pure bromine at different temperatures (80–110°C) to produce third stage compounds. Though all the compounds had the same initial stage, E_1 increased with increasing intercalation temperature. Thus, the initial stage is not the sole factor that determines the exfoliation behavior.

For all the intercalate species studied (Br_2, ICl and HNO_3), acoustic emission occurred before appreciable exfoliation took place. Figure 9 shows the acoustic emission and expansion of graphite–bromine (4 × 4 mm), which had been intercalated to 3.2 mol% Br_2 (stage 4). The acoustic emission events were observed as a large number of pulses within a short period of time. Very few events were observed once marked expansion had begun. While it may certainly have been the case that once a cellular structure began to form the acoustic pulses were attenuated beyond detection, a gradual reduction in the number of pulses was not observed. Instead, emission was observed at generally one or two distinct temperatures which were separate from the exfoliation onset temperature. In the case of graphite–Br_2, acoustic emission happened to occur during heating in the first exfoliation cycle at about the temperature of the second exfoliation.

4. DISCUSSION

We assume that the precursor of bubbles are intercalate filled penny-shaped cracks distributed within a graphite crystal. If the crystal is heated, the pressure within the cracks will increase as the intercalate takes on a more gaseous character. Higashida and Kamada[20] analyzed the stress distribution around pressurized penny-shaped cracks in graphite near a free surface and concluded that two fracture modes are available. One fracture mode is brittle fracture as a Griffiths crack, i.e. the crack diameter increases when the tensile stress in the *c*-direction exceeds the fracture strength. The other fracture mode is the buckling of the walls of the crack, i.e. when large bending moments exist at the crack tip, the flat crack may open to form a bubble. We propose that the latter fracture mode is responsible for the expansion observed in exfoliation. Higashida and Kamada found that the internal pressure necessary for fracture by either mode increased as the crack diameter decreased, though propagation of a Griffiths crack was favored in small diameter cracks and buckling was favored for large diameter cracks. Our observation of acoustic emission well before exfoliation suggests that the penny-shaped cracks do propagate initially as Griffiths cracks, with very little net expansion, then fracture by buckling to produce exfoliation.

One possibility for the source of the penny-shaped cracks is defects either pre-existing in the graphite or caused by the intercalating conditions. If pre-existing defects serve as sites for penny-shaped cracks, one might expect the exfoliation behavior to be affected mainly by differences in defect distribution due to the graphitizing process. Once the defects have become saturated with intercalate, there should be little dependence of exfoliation on stage or intercalate concentration. If the defects are not saturated, there should be an intercalate concentration dependence, i.e. with less intercalate, less expansion. If defects produced during intercalation serve as crack sites, one would expect that more severe intercalating conditions should produce more defects, hence more exfoliation. Consequently one would expect a low stage compound to be associated with more defects and a greater degree of exfoliation. Otherwise, for saturated defects only a weak dependence on concentration should be expected.

Unfortunately, none of these arguments for exfoliation from either pre-existing or induced defects is supported by what we have observed in intercalated graphite. If preexisting defects aid exfoliation, one might expect more exfoliation in a more defective graphite. In fact, fibers, which may be expected to have the greatest density of pores and defects, exfoliate the least[17], while single crystal flakes, which may be considered more perfect than HOPG, exfoliate the most[17]. On the other hand, if the defect

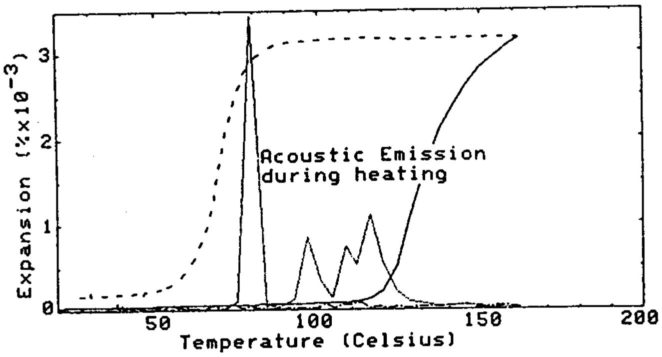

Fig. 9. Acoustic emission vs temperature superimposed on a curve of fractional expansion vs temperature for one exfoliation-collapse cycle of graphite–Br_2 (HOPG), which had been intercalated to 3.2 mol% Br_2.

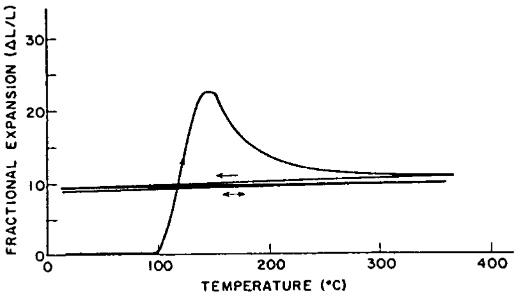

Fig. 10. Fractional expansion vs temperature during the first two exfoliation-collapse cycles of graphite–nitric acid (HOPG).

Table 4. Exfoliation behavior of parent third stage graphite–bromine prepared at various temperatures

Intercalation Temperature (°C)	Fractional Expansion (E_1)(ΔL/L)
80	16 ± 5
90	24 ± 5
100	29 ± 6
110	38 ± 6

sites are the result of the intercalation process, one might expect that a more vigorous intercalation process should produce a greater degree of exfoliation. Again, what is observed is that graphite–ICl and graphite–HNO_3 exfoliate on heating to a lesser degree than graphite–Br_2, though both intercalate to first stage and are known to cause cracking and exfoliation during intercalation. Even considering just the graphite–Br_2 system, third and fourth stage samples exfoliate to a greater degree than second stage though intercalation to either third or fourth stage may be considered milder than to second stage and certainly are slower.

We propose that the intercalate islands, suggested by Daumas and Herold[21], determine the size of the penny-shaped cracks. (The crack size is not necessarily equal to the island size; instead we expect a positive correlation between the island size and the subsequent crack size.) In turn, the size of the intercalate islands is determined by the intercalating conditions. In accordance with nucleation theory, as the reactant activity increases, competition between nucleation sites increases and the subsequent microstructure is finer. Hence, as the intercalate activity is decreased, by dilution or by heating, the intercalate island size is expected to increase. For a compound of a given concentration, increased island size means that exfoliation can occur more easily and to a greater extent. Observation of intercalate islands by electron microscopy[22, 23] shows that the intercalate islands can be treated as interstitial dislocation loops and as such are susceptible to pinning at defect sites. Nonetheless, the islands are mobile and can coalesce.

The discussion thus far tacitly assumes that the cracks are gas tight, with no net flux in or out. This is not necessarily the case. If the intercalate mobility and solubility are high, the intercalate species may diffuse out of the gas bubbles and into the matrix in a short time in comparison with the length of time required for the exfoliation cycle. For exfoliation at normal pressures, the loss of intercalate from the gas bubbles may even result in the collapse of the exfoliated structure. Subsequent heating and cooling will then cause negligible expansion. Such collapse during heating in the first exfoliation cycle was observed in graphite–nitric acid, which was prepared by immersion of HOPG (4 x 4 mm) in red fuming nitric acid (Fig. 10). When diffusion is slower, as in the case of bromine, long periods of time and high temperatures are necessary before appreciable collapse occurs (Fig. 8).

When the intercalating activity was reduced by dilution, as in the initially fourth stage samples listed in Table 3, we observed that the amount of exfoliation was greater than that of an initially second stage sample, even though the actual concentration was approximately the same for various samples. Similarly, if the activity is decreased by heating, the amount of exfoliation was observed to increase with temperature for a given stage (Table 4).

Let us consider the effect of desorption on exfoliation. Bardhan *et al.*[24] showed that a pronounced weight loss occurred on desorbing graphite–Br_2. Isothermal gravimetric results[24] indicate that desorption reduces the concentration to a limiting value of ~1.0–1.5 mol% Br_2, up to the temperature where exfoliation occurs. The mass fraction of bromine lost depends on $\sqrt{(Dt/l^2)}$, where D is the diffusion coefficient and l is half the sample width. Profilometry[24] and X-ray absorption studies[25] indicate that the concentration in a desorbing graphite–Br_2 compound decreases at the edge initially while the center retains the semblance of the undesorbed sample. By the time the apparent residue compound has been achieved, the concentration profile across the sample is nearly flat, with little difference in the concentration at the edge or the center. The length of time needed for this to occur can be considered as roughly proportional to l^2/D. Hence, for the same concentration, a sample half as wide as a given sample will require roughly a quarter of the time to desorb to an equivalent concentration.

The above argument applies to exfoliation in the following manner. During exfoliation the temperature is steadily rising rather than being isothermal. Consequently the diffusion coefficient should be considered as a composite diffusion coefficient weighted by the mass loss rate at each temperature. In effect, small samples may desorb to a low or even residue concentration during the heating cycle though they may have been concentrated or even saturated prior to heating. In this case the exfoliation behavior will be the same for an initially desorbed sample as for an initially saturated sample. Experimentally this was observed, as shown by the

3 mm sample shown in Fig. 6. For wider samples, a more and more significant amount of intercalate remains in the center of the sample by the time the exfoliation temperature is reached, with the result that the amount of exfoliation increases as the sample width increases. This is the situation described by the solid circles in Fig. 6. On the other hand, if the samples have been desorbed to a low or residue composition prior to exfoliation, this width dependence becomes negligible, as shown by the open circles in Fig. 6. For the same heating rate, as was the case for all the samples in Fig. 6, the effective (Dt) term is the same for all the samples, so that the intercalate concentration remaining in a large sample at the exfoliation temperature is greater than that in a small sample for the case of initially concentrated samples. Therefore the amount of exfoliation increases with sample width for initially concentrated samples, as we have observed.

The mobility of the intercalate is quite high at the exfoliation temperatures, and the solubility of the intercalate appears to be quite low. Diffusion of the intercalate out of the sample through the matrix is one mechanism for the loss of excess intercalate and is suggested by the least square fit of the data in Fig. 5. However, it is not necessarily the only mechanism. The gas cells themselves may serve as sinks for the excess intercalate. Under such circumstances, the matrix would lose intercalate while the sample as a whole would not. On subsequent exfoliation cycles the enriched cells should expand to a greater degree. The latter possibility is consistent with the observation of $E_2 > E_1$ for samples which are initially desorbed. The diffusion of the intercalate out of the sample is not the only means of losing intercalate. It should be borne in mind that the weight losses during the first two exfoliation cycles in Fig. 5 do not fit the least square line. There is considerably more desorption during these two cycles than can be explained by using the same diffusion coefficient which can be applied to the later cycles. It seems far more likely that a certain number of the gas bubbles present are bursting, or are forming an interconnected network which in turn opens to the outside of the sample. The channels suggested by Dowell[7] may be such a network. If so, one would expect that a greater initial concentration would tend to rupture and/or interconnect more of the cells, as a greater concentration would serve as a source of a greater gas volume. Consequently a greater proportion of the initial concentration would be lost on the first exfoliation cycle of an initially concentrated sample than in one which had been desorbed prior to exfoliation. With such a loss of intercalate, less is available on subsequent cycles so that the amount of exfoliation is decreased as shown by the solid circles in Fig. 4.

Table 5 shows the comparison of the exfoliation temperatures (first onset temperatures) of graphite–HNO_3, graphite–Br_2, and graphite–ICl with the respective intercalate melting temperatures and the respective melting and boiling points of bulk HNO_3, Br_2 and ICl. For graphite–Br_2, the collapse temperature (which is the same as the second exfoliation temperature) is approximately the same as the intercalate melting temperature. Other than this match, the exfoliation and collapse temperatures are different from any of the corresponding critical temperatures listed. Comparison of the trends down the various columns in Table 5 shows a possible relationship between the exfoliation temperature and the bulk melting temperature.

5. CONCLUSION

The amount of exfoliation of graphite–Br_2 was found to be determined by the intercalation conditions, namely the Br_2 concentration in the Br_2–CCl_4 solution and the temperature, such that the expansion increased with increasing initial stage number and with increasing temperature. Due to intercalate desorption during heating, annealing was found to increase the amount of residual expansion until exfoliation became irreversible. Desorption also resulted in the increase of the exfoliation expansion with increasing sample width for concentrated samples and the decrease in the expansion with repeated exfoliation cycles for these samples. A single exfoliation event was found to consist of multiple expansion spurts, which occurred at ~150 and ~240°C for first exfoliation, and at ~100 and ~240°C for subsequent cycles. Acoustic emission was observed before appreciable expansion during the first exfoliation cycle. In-plane intercalate order-

Table 5. Comparison of acoustic emission, exfoliation and collapse temperatures with other critical temperatures

Intercalate Species	Acoustic emission temperature (±10°C)	Exfoliation temperature* (±20°C)	Collapse temperature (±10°C)	Intercalate melting temperature (°C)	Bulk melting temperature (°C)	Bulk boiling temperature (°C)
HNO_3	80	130	/	-20	-42	83
Br_2	115	170	100†/210‡	101	-7	59
ICl	140	190	190	41	14§/27**	97

* First onset temperature (T_1)

† For HOPG

‡. For single crystal graphite

§ For β-ICl

** For α-ICl

ing was observed by X-ray diffraction in exfoliated graphite–Br_2. A model of exfoliation involving intercalate islands[21] is proposed.

Acknowledgements—The authors are grateful to Mr. H. H. Lee of Carnegie-Mellon University for assistance in the acoustic emission measurement and to Prof. Roy Clarke of the University of Michigan for providing natural graphite flakes. The X-ray diffraction equipment grant from the Division of Materials Research of the National Science Foundation under Grant No. DMR-8005380 is acknowledged. Support from the Materials Research Laboratory Section, Division of Materials Research, National Science Foundation under Grant No. DMR 76-81561 A01 is also acknowledged.

REFERENCES

1. J. E. Brocklehurst, *Nature* (*London*) **194**, 247 (1962).
2. W. H. Martin and J. E. Brocklehurst, *Carbon* **1**, 133 (1964).
3. A. R. Ubbelohde, *Brit. Coal Util. Res. Assoc. Gaz.* **51**, 1 (1964).
4. C. Mazieres, G. Colin, J. Jegoudez and R. Setton, *Carbon* **13**, 289 (1975).
5. C. Mazieres, G. Colin, J. Jegoudez and R. Setton, *Carbon* **14**, 176 (1976).
6. R. E. Stevens, S. Ross and S. P. Wesson, *Carbon* **11**, 525 (1973).
7. M. B. Dowell, *Ext. Abs. Program*, 12*th Bienn. Conf. Carbon*, p. 31. American Carbon Society (1975).
8. H. Thiele, *Anorg. Allgem. Chem.* **207**, 340 (1932).
9. M. B. Dowell, *Ext. Abs. Program*, 12*th Bienn. Conf. Carbon*, p. 35. American Carbon Society (1975).
10. Union Carbide Trademark, U.S. Pat. 3,404,061 (1968).
11. H. Mikami, Kokai (Japan Pat. 76 96,793 (1976).
12. CECA S. A., Carbone-Lorraine S. A., Brit. Pat. 1,588,876.
13. W. L. Garrett, J. Sharma, J. Pinto and H. Prask, *Technical Report ARLCD-TR*-81008, AD-E400 617; Order No. AD-A100727 (May 1981) 16, Avail. NTIS.
14. M. A. M. Boersma, In *Adv. Mater. Catal.* (Edited by J. Burton and R. L. Garten), p. 67. Academic Press, New York (1977).
15. K. Aoki, T. Hirai and S. Yajima, *J. Mat. Sci.* **6**, 140 (1971).
16. L. C. Olsen, S. E. Seeman and H. W. Scott, *Carbon* **8**, 85 (1970).
17. S. H. Anderson and D. D. L. Chung, *Synth. Met.* **8**, 343 (1984).
18. S. H. Anderson, H. H. Lee and D. D. L. Chung, *Ext. Abs. Program*, 15*th Bienn. Conf. Carbon*, p. 357. American Carbon Society (1981).
19. D. Ghosh and D. D. L. Chung, *Mater. Res. Bull.* **18**, 727 (1983).
20. Y. Higashida and K. Kamada, *J. Nucl. Mater.* **73**, 30, 41 (1978).
21. N. Daumas and A. Herold, *C. R. Acad. Sci.* (*Paris*), *Ser.* **C268**, 373 (1969).
22. M. Heerschap, P. Delavignette and S. Amelinckx, *Carbon* **1**, 235 (1964).
23. M. Heerschap and P. Delavignette, *Carbon* **5**, 383 (1967).
24. K. K. Bardhan, J. C. Wu, J. S. Culik, S. H. Anderson and D. D. L. Chung, *Synth. Met.* **2**, 57 (1980).
25. S. H. Anderson and D. D. L. Chung, *Ext. Abs. Program*, 15*th Bienn. Conf. Carbon*, p. 361. American Carbon Society (1981).